Journal of Materials Chemistry A

Accepted Manuscript

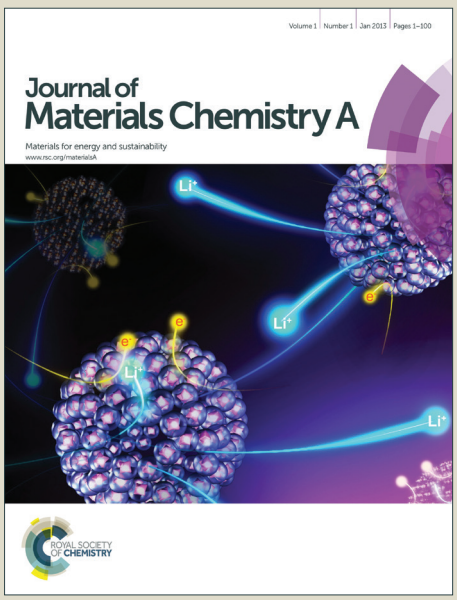

ROYAL SOCIETY OF CHEMISTRY

www.rsc.org/materialsA

Journal of Materials Chemistry A

RSCPublishing

COMMUNICATION

Bio-derived calcite as a sustainable source for graphenes as high-performance electrode material for energy storage

Cite this: DOI: 10.1039/x0xx00000x

Huang Tang,[a,b] Peibo Gao,[a] Xianmin Liu,[a] Huanguang Zhu[a] and Zhihao Bao*[a]

Received 00th xxxxxx 2014,
Accepted 00th xxxxxx 2014

DOI: 10.1039/x0xx00000x

www.rsc.org/

Graphenes are promising materials for the energy conversion and storage applications. However, the production of graphenes was limited by their complicated high-cost processing. Here we showed that graphenes could be synthesized by a simple magnesiothermic reduction reaction from eggshell, a sustainable precursor of bio-calcite produced at a rate of tens of millions of tons annually. Due to their intrinsic structure (e. g., porous structure, high crystallinity), the synthesized graphenes could be used as a promising electrode material with high-capacity, high-rate capability and long cyclability. At a specific current of 100 mA g^{-1}, they exhibited a reversible capacity of 678.4 mA h g^{-1}. Even at an extremely high discharge/charge current of 20 A g^{-1} (about 27 s to full charge), it retained a capacity of 149.9 mA h g^{-1} after 1000 charge/discharge cycles. At such rate, it could exhibit a specific energy density of 253.9 W h kg^{-1} and a specific power density of 32.6 kW kg^{-1}. Above results suggested that bio-calcite derived from eggshell could be a sustainable and ample resource to synthesize graphenes for energy storage.

Graphene is a single sheet of sp^2 bonded carbon atoms arranged in a 2-dimensional (2D) hexagonal structure.[1] The structure enables graphene exhibit unique chemical, physical and mechanical properties.[2-4] Besides monolayer graphene, there are few-layer and multi-layer graphenes. They have advantages in the applications for energy conversion and storage compared with traditional carbon materials.[4-8] For example, Li ions can be stored on both sides of monolayer graphene to form LiC_3 structure.[9] Thus, the monolayer graphene can achieve a theoretical capacity of 744 mA h g^{-1}, two times of graphite's, 372 mA h g^{-1}.[10, 11] Graphenes with relatively perfect structure were fabricated with mechanical exfoliation,[1] chemical vapor deposition (CVD),[12, 13] epitaxial growth[14, 15] and unzipping of carbon nanotube.[16] However, the production rate of graphenes via the above methods was limited. Large quantities of graphenes could possibly be obtained through the reduction of graphene oxide,[17-20] which was synthesized by Hummer's[21] or modified Hummer's methods.[22, 23] However, above methods required strong oxidizers such as sodium nitrate and potassium permanganate. Meanwhile, the reducing agents such as hydrazine,[20] sodium borohydride[24] and hydroiodic acid[25] were toxic. The graphene product from the reduction of graphene oxide also exhibited low ratio (<15) of carbon and oxygen, and poor conductivity.[26] Recently, magnesium (liquid/vapor) emerged as a powerful reducing agent. Our previous research work demonstrated that silicon oxide could be reduced into nanostructured silicon.[27, 28] Most recently, the nanostructured carbon product was synthesized by directly burning magnesium in flowing carbon dioxide.[29] However, the carbon product exhibited poor crystallinity with a low intensity ratio of G and D band in the Raman spectra. It might be due to the activation of the reduced carbon materials by the surplus carbon dioxide. Herein, we proposed a magnesiothermic reduction process with a controlled ratio of reactants to synthesize graphene materials with high crystallinity by using the bio-derived calcite from eggshell as precursor. The great potential of the synthesized graphene materials as high-performance electrode material was also demonstrated. The reversible capacities of synthesized graphene could reach 678.4 mA h g^{-1}, superior to most of graphene materials. At a discharge/charge rate as high as 20 A g^{-1}, the graphene-based electrode material could still retain a capacity of 149.9 mA h g^{-1} even after 1000 discharge/charge cycles. It could exhibit a specific energy density of 253.9 W h kg^{-1} and a specific power density of 32.6 kW kg^{-1}.

The new proposed process was shown in the flow chart in Fig. 1, in which bio-calcite derived from eggshell was used as a sustainable source to generate carbon dioxide at relatively high temperature (600-800 °C). Then it was reduced into graphene materials by the magnesiothermic reduction reaction. The impurity in the product was etched away by hydrochloric acid. The proposed process has following advantages (i) precursors of bio-derived calcites (e.g., eggshell, crab-shell) are ample and sustainable. In China, ~27 million tons of eggs are yielded

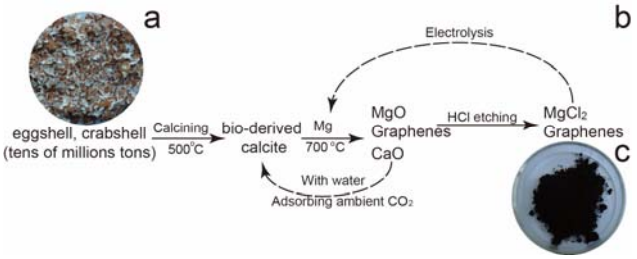

Figure 1. A process to synthesize graphenes from the bio-calcite precursors such as eggshell and crab shell. (a) Optical image of the eggshell, (b) flow chart of the process and (c) optical image of the graphene product.

annually,[30] generating about 2.7 million tons of calcite (note: ~10% of the whole weight of an egg is from eggshell).[31] If 10% of carbon element inside them could be converted into graphene materials, the yield can reach 0.32 million tons, which can meet the entire need for the electrode materials (~10^5 tons) in the world. (ii) The bio-calcite as a solid reservoir for gaseous CO_2 can be easily used to adjust its ratio to Mg to guarantee that formed graphenes are always in the reducing atmosphere for good crystallinity. Such bio-derived calcite with nanostructures can also decompose at a lower temperature compared with the bulk one, which makes it possible to control the morphology and structure of graphene product by adjusting the reaction temperature in a large range. (iii) The reducing agent, Mg, is one of the most commonly used metal. It can be recycled from the by-product of the process, $MgCl_2$, by electrolysis. Meanwhile, the other by-product, calcium oxide, can easily react with water to form calcium hydroxide to adsorb greenhouse gas (CO_2) from ambient atmosphere and turn into calcium carbonate, which can be reused as the precursor of carbon dioxide. In all, the overall process is scalable and sustainable.

To obtain bio-derived calcite, eggshell was first calcined at 500 °C for 2 h in air to remove organic components. X-ray diffraction (XRD) pattern (Fig. 2a) of the calcined product showed that it was of calcite nanocrystallites with an average size of 29.1 nm estimated by Scherrer equation. Thermogravimetric analysis (TGA; Fig. 2b) revealed that the product began to lose weight at 624 °C and stopped at 816 °C. Calcium carbonate was estimated to account for 94.6% of the overall weight of the calcined eggshell, assuming impurity remained untouched in the process. Differential scanning calorimetry (DSC) analysis showed an endothermic peak for the bio-derived calcite at 780 °C, which was lower than commercial available calcite (Fig. S1) and bulk calcite's decomposition temperatures.[32] The lower decomposition temperature might be ascribed to the size effect.[33] To synthesize graphene materials, calcined eggshell and Mg flakes (mass ratio=1:1) were sealed at the two ends of a steel ampoule separately in an argon-filled glovebox. Then the ampoule was heated to 700°C with a heating rate of 5 °C/min and kept at that temperature for 5 h in an argon flow. After the ampoule was cooled down and opened, most of the black product was found to appear at the location of Mg flake. XRD analysis (Fig. S2) of the black product revealed that it contained un-reacted metallic magnesium and magnesium oxide. However, the calcined eggshell was turned into calcium oxide (XRD, Fig. S3) barely bearing black product. Combined with the results from previous studies,[29] the overall reaction at 700 °C can be expressed as below:

$$CaCO_3(s)+2Mg(l)= CaO(s) +2MgO(s)+C(s) \quad 700\ ^oC \quad (1)$$

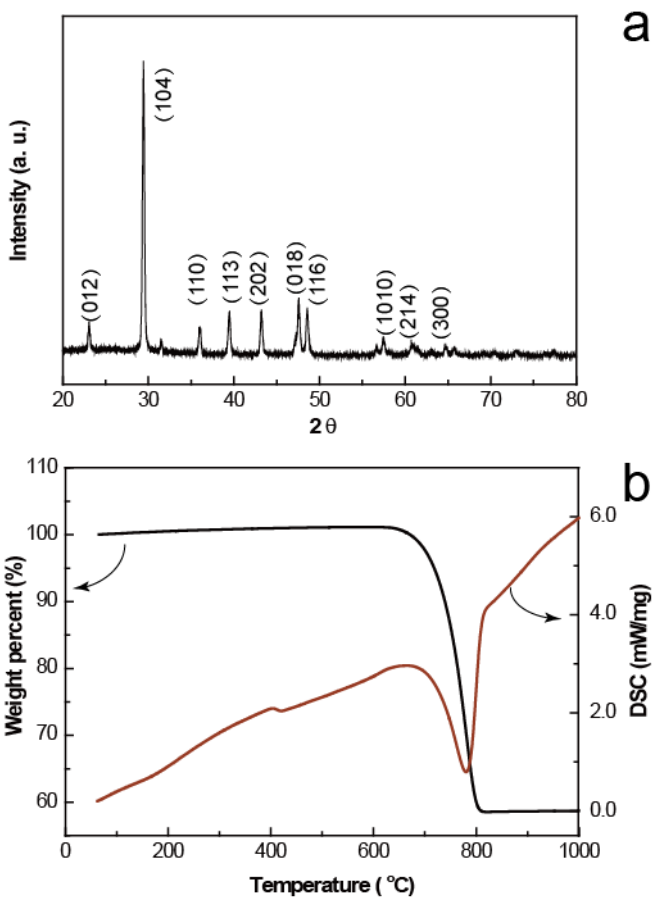

Figure 2. Characterization of bio-calcite derived from eggshell. XRD (a) and TG-DSC(b) analyses of bio-calcite derived from the eggshells.

Judging from the location of black product, we believed the decomposition of bio-derived calcite or diffusion of carbon dioxide could not be a rate-limiting step of the whole reaction. It was possible due to the appreciably higher equilibrium CO_2 pressure (0.030 atm) for the decomposition of calcium carbonate than the equilibrium magnesium vapour pressure (0.010 atm) over the liquid magnesium at 700 °C according to the thermodynamic calculation.[34] The black carbon product at the location of Mg flake was collected after the impurities such as Mg and MgO were removed by hydrochloric-acid etching. Transmission electron microscopy (TEM) images (Fig. 3) showed the microstructures of the carbon product. The cross-section images (Fig. 3a, b and c) of the product revealed that it contained graphenes with different thicknesses. The appearance of graphene nanosheets with the thickness of a few nanometers was also confirmed by the atomic force microscopy (AFM) images (Fig. S4a, b). Based on statistics (Fig. S4c) on TEM cross-section images and AFM images, the thicknesses of most of graphenes were found to be less than 10 nm. It was also found that synthesized bilayer graphene (Fig. 3a) had a larger interlayer distance of 0.37 nm than that (0.34 nm) of multilayer graphene (Fig. 3b). It was consistent with the finding in the previous study.[5] The graphene product with a large range of thicknesses was confirmed by XRD diffraction pattern (Fig. 4a). The characteristic peaks of the pattern were at 26.3 and 42.5 degree, corresponding to the diffractions from (002) basal plane

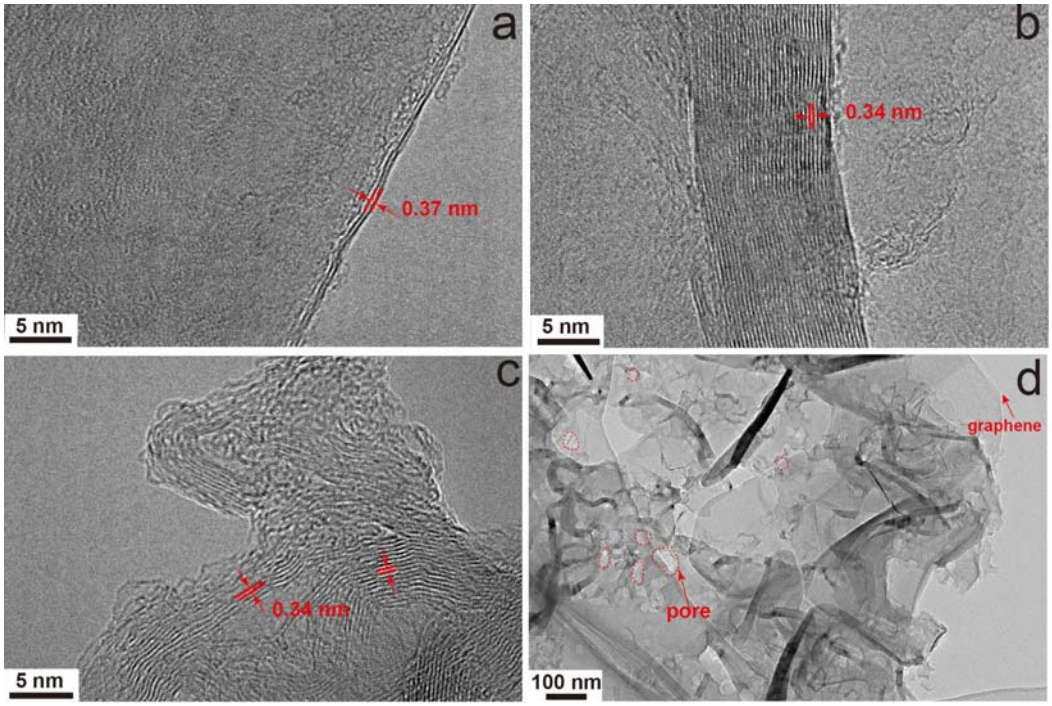

Figure 3. Representative TEM images of synthesized graphene materials. (a) and (b) graphenes with different thickness. (c) graphene aggregates with corrugated structure and (d) graphene aggregate with pores labelled with red dot line.

and (100) plane, respectively. The peak at 26.3 degree was composed of a bump background and a relatively sharp peak. The sharp peak was from multilayer graphene while the bump background could be induced by graphenes with a few layers.[35, 36] These graphenes contained pores with sizes of tens of nanometers, as indicated in TEM image (Fig. 3d). The selected area electron diffraction (SAED, Fig. S5) exhibited several sets of hexagonal spots (e.g., the one marked in the figure), confirming the formation of graphene sheets. The different sets of hexagonal spots indicated the existence of rotational stacking faults in the synthesized graphene sheets or the random overlapping of graphene sheets.[37] Fig. 4b showed the nitrogen absorption/desorption curve of synthesized graphene materials at 77 K. Based on it, the BET specific surface area (SSA) of the graphene–based materials was calculated to be 551.18 m^2 g^{-1}, equivalent to SSA of nanosheets with ~5 monoatomic graphene layer. Pore size distribution analysis (inset in Fig. 4b) based on Barrett–Joyner–Halenda (BJH) model showed that graphene product was mesoporous, which was consistent with TEM observation.[38] The Raman spectrum of graphene materials showed the peaks at 1345 and 1569 cm^{-1}, corresponding to D and G bands, respectively.[39] The ratio of peak intensities of G and D bands of synthesized grapahene materials was calculated to be 1.77, indicating good crystallinity. The peak position of 2D band at 2684 cm^{-1} was obviously downshifted compared with that (~2700 cm^{-1}) of the bulk graphite, indicating the appearance of graphenes with less than 5 monoatomic layers.[40] The XPS survey spectrum (Fig. S6) revealed that graphene product was only composed of carbon and oxygen. The C1s and O1s XPS spectra of the synthesized graphene were further shown in Fig. 4d. The C1s peak was deconvoluted into peaks at 284.6 (C-C/C=C), 286.5 (C-O) and 287.9 eV (C=O) respectively.[41] The peaks for C-O and C=O were very weak, indicating small portions of such bonds in the synthesized graphenes. The atomic ratio of carbon to oxygen (area of the C1s peak divided by area of the O1s peak, multiplied by ratio of oxygen and carbon relative sensitivity factors) was 17.2:1,[42] larger than that of most chemically reduced graphene materials.[26] The appearance oxygen element might be from oxygen-containing functional groups. The possible growth mechanism for the graphene materials was that metallic magnesium melt at the temperature above 650 °C and then CO_2 molecules were adsorbed and reduced on the surface of melt magnesium. The monolayer carbon atom and MgO formed the layer structure to minimize the surface energy. Then additional layers of carbon was grown to form the product. In the formation of graphene materials, there might be not enough carbon atom supply to form carbon islands or the Mg liquid droplets was encapsulated by

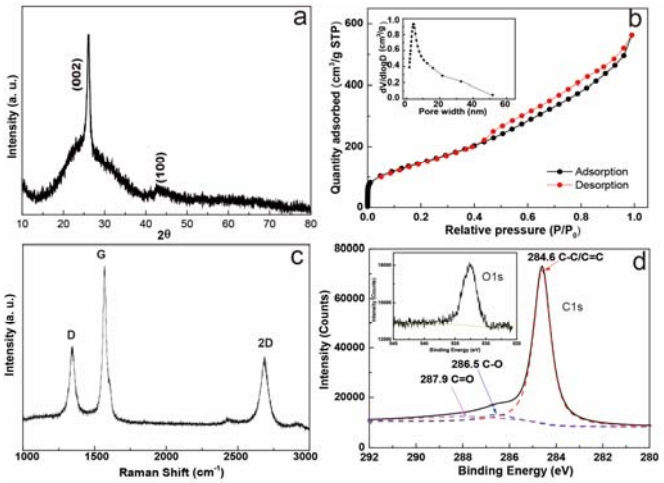

Figure 4. Characterization of the synthesized graphene product. XRD pattern (a), nitrogen isotherm absorption/desorption curve at 77 K (inset: pore size distribution)(b), Raman spectrum (c) and C1s and O1s XPS spectra (d) of the synthesized graphene product.

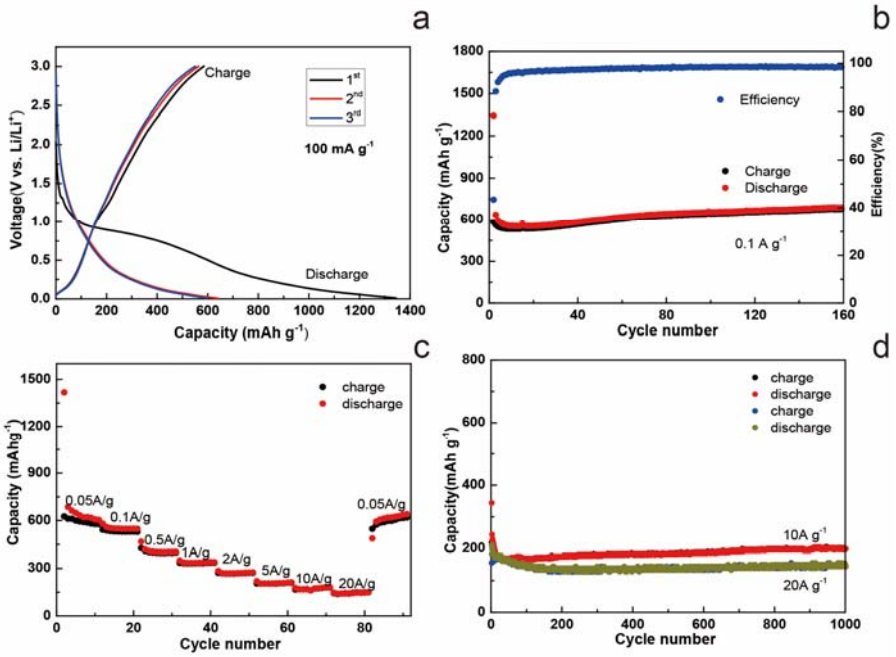

Figure 5. Electrochemical performance of the electrode base on the synthesized graphene materials. (a) Galvanostatic charge/discharge profile at the first three cycles and (b) Cycling performance at a specific current of 100 mA g^{-1} in the voltage range of 0.01-3.0 V versus Li/Li^+. (c) Rate performance in the specific current range of 0.05-20 A g^{-1}. (d) Long-term cycling performance of electrodes based on the synthesized graphene at the specific currents of 10 and 20 A g^{-1}, respectively.

layers of carbon atoms.[29] After the etching of hydrochloric acid, porous structure formed. To study the effect of the reaction temperature on the morphology and crystallinity of the carbon product, the same reduction process was conducted at 600 °C. The obtained product was amorphous porous carbon (TEM, Fig. S7) with a low intensity ratio of G band and D band (Raman spectrum, Fig. S8). At that temperature, the mobility was too low for carbon atoms to be organized into the structure with a long-range order.

To study the lithium-storage properties of the obtained graphene product. The graphene-based electrodes were cycled between 0.01-3.0 V. The electrochemical charge/discharge curves (Fig, 5a) exhibited no plateau, which was different from graphite. The absence of the plateau was due to the disordered stacking of the graphene layers with non-equivalent Li intercalation sites.[5] The reversible capacity below 0.5 V was related to the intercalation of lithium into graphene layer. While the reversible capacity above 0.5 V accounted for a large portion of the overall capacity, indicating that majority of the Li ions was stored in the defects in the basal plane and at edges.[43, 44] Such pseudo- capacitive behaviour of synthesized graphene above 0.5 V could exactly be used to store the lithium ions/energy with similar mechanism in lithium ion supercapacitors.[45,46] The first discharge capacity was 1343.6 mA h g^{-1} and the corresponding charge capacity was 584.1 mA h g^{-1} with a low Coloumbic efficiency of 43.5%. The low Coloumbic efficiency was due to irreversible reactions of lithium ions with surface defects such as point defects or oxygen containing functional groups. The cyclic voltammogram (CV) curves of the synthesized graphene were shown in Fig. S9. The CV curves did not exhibit sharp anodic and cathodic peaks, which was consistent with the absence of the plateau in the charge/discharge profiles. In the first cycle, a broad cathodic peak appeared near 0.35 V can be ascribed to defect-associated lithium adsorption,[47] while the broad peak at 1.12 V could be attributed to formation of SEI film. Fig. 5b showed the cycling performance of the graphene-based electrode at a specific current of 100 mA g^{-1}. Its capacity first dropped and then gradually increased. Such capacity fluctuation in graphene electrode was also reported by the previous study, which suggested that it was due to the side reactions between the electrolyte and the active sites of oxygen-containing functional groups.[7] After stabilization, the electrode exhibited good cycling performance. Coulombic efficiency was also increased to 96.0% after 10 cycles. After 160 cycles, it still retained a capacity of 678.4 mA h g^{-1}. The capacity was superior to most of reported graphene materials, which were summarized in Table S2. Rate capability of graphene material-based electrode was shown in Fig. 5c. Under the specific discharge/charge densities of, 0.5, 1, 2, 5, 10 and 20 A g^{-1}, the reversible capacities were 398.6, 335.8 ,272.0, 209.6, 181.1 and 149.8 mA h g^{-1}, respectively. Such excellent rate performance suggested that the graphene-based electrodes could be fully charged very quickly. For example, at a very high specific current of 20 A g^{-1}, it took ~27 s to fully charge the graphene based cell. Our graphene based electrode also exhibited long-term cyclability (Fig. 5d). After 1000 charge/discharge cycles, the reversible capacity can still retained 190 mA h g^{-1} and 149.9 mA h g^{-1}, at the specific current of 10 and 20 A g^{-1}, respectively. Such excellent rate-capability made it possible to use synthesized graphene as high-power electrode material.

To evaluate the their possibility used in high-power applications, the energy density and the average power density of graphene materials at the constant charge/discharge currents were estimated by using the following equations:

$$E = \frac{I}{m}\int_0^t V dt \quad (2)$$

$$P = \frac{E}{t} \quad (3)$$

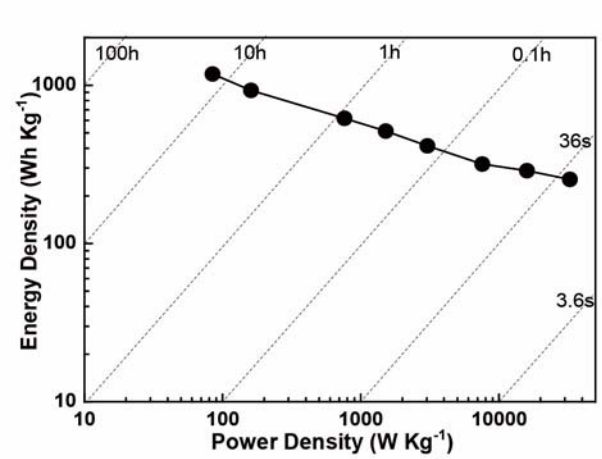

Figure 6. Ragone plot for the synthesized graphene. The calculation was based on the active graphene mass with metallic lithium as the counter electrode.

where I, m, V and t are the current, mass of active material, voltage and the charge time, respectively. Based on the above equation, the energy and power density were calculated and shown in Ragone plot (Fig. 6). At a high charge rate 0.5 A g^{-1}, the energy density and powder density were calculated to 617.4 W h kg^{-1} and 762.5 W kg^{-1}, respectively. The energy density and power density of the graphene materials were 288.4 W h kg^{-1}, 16.0 kW kg^{-1} and 253.9 W h kg^{-1}, 32.6 kW kg^{-1} at higher charge/discharge rate of 10 A g^{-1} and 20 A g^{-1}, respectively. These values were higher than energy and power densities of reported graphene electrodes and comparable to the doped-graphene electrodes.[7] The superior rate performance and relatively high energy density of the graphene based cell are desirable for high-power applications, where supercapacitor was usually used. We believed the intrinsic structure of the synthesized graphenes was responsible for their good electrochemical properties. The large interlayer distance for graphene nanosheets with a few monatomic graphene layers might increase the accommodation number of lithium ions. At the same time, the appearance of pore structure could also increase the number of edge defects for reversible storage of lithium ions. Meanwhile, all the synthesized graphene materials were of nano-dimensions, which guaranteed that lithium ions moved into/out the interlayer space more easily compared to the bulk materials. The pore structure existed in the graphene materials enabled lithium ions quickly transport for superior rate performance and increased power density of the graphene-based electrode. At the same time, the good crystallinity of the graphenes could enhance the transportation of electrons.

Apart from the eggshell, we also successfully utilized the bio-calcite from the crab shell, another abundant resource, to obtain the graphene materials with the same magnesiothermic reduction process. Thus, the natural and sustainable bio-calcite sources such as eggshell and crab shell provide a low-cost and environmentally benign source for nanostructured electrode material.

Conclusions

The present study demonstrates that the bio-derived calcites from eggshell and crab shell can be used to produce nanostructured graphene materials with the magnesiothermic reduction reaction. Moreover, the porous structure, good crystallinity and increased interlayer distance enabled that graphene materials exhibited excellent electrochemical performance as LIB electrode. In addition to LIBs, the nanostructured graphene materials can find other potential applications such as electrode material for supercapacitors and conductive carbon material, providing great demand on them. Given that annual bio-calcite production can reach tens of millions of tons, the simple, scalable and low-cost process introduced in this study can possibly meet such demand on graphene materials.

Acknowledgements

This work was supported by the Scientific Research Foundation for Returned Scholars, the Ministry of Education of China, Key Basic Research Projects of Science and Technology Commission of Shanghai (No. 11JC1412900), and the National Science Foundation of China program (No. 21271140).

Notes and references

[a] Shanghai Key Laboratory of Special Artificial Microstructure Materials and Technology, School of Physics Science and Engineering, Tongji University, 1239 Siping Road, Shanghai 200092, China. Email: zbao@tongji.edu.cn

[b] School of Mathematics and Physics, Jiangsu University of Technology, 1801 Zhongwu Road, Changzhou 213001, China

† Electronic Supplementary Information (ESI) available. See DOI: 10.1039/c000000x/

1 K. S. Novoselov, A. K. Geim, S. V. Morozov, D. Jiang, Y. Zhang, S. V. Dubonos, I. V. Grigorieva and A. A. Firsov, Science, 2004, 306, 666.
2 C. Lee, X. D. Wei, J. W. Kysar and J. Hone, Science, 2008, 321, 385.
3 A. A. Balandin, S. Ghosh, W. Z. Bao, I. Calizo, D. Teweldebrhan, F. Miao and C. N. Lau, Nano Lett., 2008, 8, 902.
4 Y. W. Zhu, S. Murali, M. D. Stoller, K. J. Ganesh, W. W. Cai, P. J. Ferreira, A. Pirkle, R. M. Wallace, K. A. Cychosz, M. Thommes, D. Su, E. A. Stach and R. S. Ruoff, Science, 2011, 332, 1537.
5 E. Yoo, J. Kim, E. Hosono, H. Zhou, T. Kudo and I. Honma, Nano Lett., 2008, 8, 2277.
6 H. L. Wang, L. F. Cui, Y. A. Yang, H. S. Casalongue, J. T. Robinson, Y. Y. Liang, Y. Cui and H. J. Dai, J. Am. Chem. Soc., 2010, 132, 13978.
7 Z. S. Wu, W. C. Ren, L. Xu, F. Li and H. M. Cheng, ACS Nano, 2011, 5, 5463.
8 X. W. Yang, C. Cheng, Y. F. Wang, L. Qiu and D. Li, Science, 2013, 341, 534.
9 G. Wang, B. Wang, X. Wang, J. Park, S. Dou, H. Ahn and K. Kim, J. Mater. Chem., 2009, 19, 8378.
10 L. Kavan, Chem. Rev., 1997, 97, 3061.
11 M. S. Whittingham, Chem. Rev., 2004, 104, 4271.
12 K. S. Kim, Y. Zhao, H. Jang, S. Y. Lee, J. M. Kim, J. H. Ahn, P. Kim, J. Y. Choi and B. H. Hong, Nature, 2009, 457, 706.
13 S. Bae, H. Kim, Y. Lee, X. F. Xu, J. S. Park, Y. Zheng, J. Balakrishnan, T. Lei, H. R. Kim, Y. I. Song, Y. J. Kim, K. S. Kim, B. Ozyilmaz, J. H. Ahn, B. H. Hong and S. Iijima, Nat. Nanotechnol., 2010, 5, 574.
14 C. Berger, Z. M. Song, X. B. Li, X. S. Wu, N. Brown, C. Naud, D. Mayou, T. B. Li, J. Hass, A. N. Marchenkov, E. H. Conrad, P. N. First and W. A. de Heer, Science, 2006, 312, 1191.

15 J. Wintterlin and M. L. Bocquet, Surf. Sci., 2009, 603, 1841.
16 D. V. Kosynkin, A. L. Higginbotham, A. Sinitskii, J. R. Lomeda, A. Dimiev, B. K. Price and J. M. Tour, Nature, 2009, 458, 872.
17 M. J. McAllister, J. L. Li, D. H. Adamson, H. C. Schniepp, A. A. Abdala, J. Liu, M. Herrera-Alonso, D. L. Milius, R. Car, R. K. Prud'homme and I. A. Aksay, Chem. Mater., 2007, 19, 4396.
18 H. M. A. Hassan, V. Abdelsayed, A. Khder, K. M. AbouZeid, J. Terner, M. S. El-Shall, S. I. Al-Resayes and A. A. El-Azhary, J. Mater. Chem., 2009, 19, 3832.
19 G. Williams, B. Seger and P. V. Kamat, ACS Nano, 2008, 2, 1487.
20 S. Stankovich, D. A. Dikin, R. D. Piner, K. A. Kohlhaas, A. Kleinhammes, Y. Jia, Y. Wu, S. T. Nguyen and R. S. Ruoff, Carbon, 2007, 45, 1558.
21 W. S. Hummers Jr and R. E. Offeman, J. Am. Chem. Soc., 1958, 80, 1339.
22 N. I. Kovtyukhova, P. J. Ollivier, B. R. Martin, T. E. Mallouk, S. A. Chizhik, E. V. Buzaneva and A. D. Gorchinskiy, Chem. Mater., 1999, 11, 771.
23 J. P. Zhao, S. F. Pei, W. C. Ren, L. B. Gao and H. M. Cheng, ACS Nano, 2010, 4, 5245.
24 H. J. Shin, K. K. Kim, A. Benayad, S. M. Yoon, H. K. Park, I. S. Jung, M. H. Jin, H. K. Jeong, J. M. Kim, J. Y. Choi and Y. H. Lee, Adv. Func. Mater., 2009, 19, 1987.
25 I. K. Moon, J. Lee, R. S. Ruoff and H. Lee, Nat. Commun., 2010, 1, 73.
26 S. F. Pei and H. M. Cheng, Carbon, 2012, 50, 3210.
27 Z. H. Bao, M. R. Weatherspoon, S. Shian, Y. Cai, P. D. Graham, S. M. Allan, G. Ahmad, M. B. Dickerson, B. C. Church, Z. T. Kang, H. W. Abernathy, C. J. Summers, M. L. Liu and K. H. Sandhage, Nature, 2007, 446, 172.
28 A. Xing, J. Zhang, Z. Bao, Y. Mei, A. S. Gordin and K. H. Sandhage, Chem. Commun., 2013, 49, 6743.
29 H. Zhang, X. Zhang, X. Sun and Y. Ma, Sci. Rep., 2013, 3, 3543.
30 Overview on China's Animal Husbandry, http://english.agri.gov.cn/overview/201301/t20130128_10651.htm.
31 P. Hunton, Braz. J. Poutry. Sci., 2005, 7, 67.
32 J. A. Dean, Lange's handbook of Chemistry, McGraw-Hill Book Co., 1999.
33 L. Yue and Z. Xu, Thermochim. Acta., 1999, 335, 121.
34 I. Barin and G. Platzki, Thermochemical data of pure substances, VCH Weinheim, 1995.
35 A. Chakrabarti, J. Lu, J. C. Skrabutenas, T. Xu, Z. L. Xiao, J. A. Maguire and N. S. Hosmane, J. Mater. Chem., 2011, 21, 9491.
36 H. Feng, R. Cheng, X. Zhao, X. Duan and J. Li, Nat. Commun., 2013, 4, 1539.
37 J. H. Warner, M. H. Rummeli, T. Gemming, B. Buchner and G. A. D. Briggs, *Nano Letters*, 2009, **9**, 102-106
38 E. P. Barrett, L. G. Joyner and P. P. Halenda, J. Am. Chem. Soc., 1951, 73, 373.
39 F. Tuinstra and J. L. Koenig, J. Chem. Phys., 1970, 53, 1126.
40 A. C. Ferrari, J. C. Meyer, V. Scardaci, C. Casiraghi, M. Lazzeri, F. Mauri, S. Piscanec, D. Jiang, K. S. Novoselov, S. Roth and A. K. Geim, Phys. Rev. Lett., 2006, 97, 187401.
41 T. Chiang, F. Seitz, Ann. Phys., 2001, 10, 61.
42 P. Seah, Auger and X-ray Photoelectron Spectroscopy, John Wiley & Sons Ltd., 1990,.
43 J. Hu, H. Li and X. Huang, Solid State Ionics, 2007, 178, 265.
44 D. Pan, S. Wang, B. Zhao, M. Wu, H. Zhang, Y. Wang and Z. Jiao, Chem. Mater., 2009, 21, 3136.
45 M. D. Stoller, S. Murali, N. Quarles, Y. Zhu, J. R. Potts, X. Zhu, H. Ha and R. S. Ruoff, Phys. Chem. Chem. Phys., 2012, 14, 3388.
46 R. Han, W. Ma, S. Pang, Q. Kong, J. Yao, C. Bi and G Cui, J. Mater. Chem. A, 2013, 1, 5949.
47 F. Yao, F. Güneş, H. Q. Ta, S. M. Lee, S. J. Chae, K. Y. Sheem, C. S. Cojocaru, S. S. Xie and Y. H. Lee, J. Am. Chem. Soc., 2012, 134, 8646

Table of contents.

Bio-derived calcite as a sustainable source for graphenes as high-performance electrode material for energy storage

Huang Tang, Peibo Gao, Xianmin Liu, Huanguang Zhu and Zhihao Bao

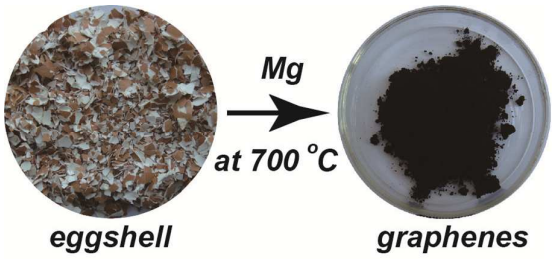

Graphenes as high-performance electrode material for energy storage were synthesized from eggshell by a magnesiothermic reduction process.